

## Chapter 5

# Detection and Attribution

Serge Planton, Armineh Barkhordarian, Aurélien Ribes,  
and Hans Von Storch

**Abstract** We present a first assessment of the detection of a signal of temperature change over the Mediterranean domain, using HadCRUT3v observation dataset and model outputs from the CMIP3 climate simulations. For this study we have used two new formal detection methodologies, the ‘Regularized Optimal Fingerprint’ and the ‘Temporal Optimal Detection’, developed within the context of the CIRCE project and aiming at improving the ability to detect a climate change signal at the regional scale. We have also applied the ‘Consistency’ method that allows to answer the question whether a given forcing is a plausible explanation of an observed change. The results show the detection of a change on spatially centered temperatures, that allows to identify a regional structure of change additional to the global warming. The formal detection findings also extend to the winter and summer spatial patterns of temperature change. By applying the ‘Consistency’ method, we also detect the GS (Greenhouse gases and Sulfate aerosol) signal in observed annual and seasonal area-mean warming except in winter. Further we find that the recent trends in near-surface temperature are significantly consistent with the simulated GS patterns. Concerning precipitation, we cannot detect formally a signal of climate change on Mediterranean precipitation using 17 series of monthly precipitation from Croatian, French and Italian coastal stations and the CMIP3 climate simulations. However this may be due, at least partly, to the limited extent of the region covered with the precipitation series.

**Keywords** Attribution • Change • Detection • Precipitation • Temperature

---

S. Planton (✉) • A. Ribes  
Group de Météorologie de Grand Echelle et Climat CNRM-GAME,  
Météo-France and CNRS, Toulouse, France  
e-mail: serge.planton@meteo.fr

A. Barkhordarian • H. Von Storch  
Institute for Coastal Research, GKSS, Geesthacht, Germany

## 5.1 Introduction

According to the IPCC third assessment report (IPCC 2001), 'detection is the process of demonstrating that an observed change is significantly different (in a statistical sense) than can be explained by natural internal variability'. The detection of climate change at the regional scale, and moreover the attribution of its causes, remain a difficult scientific issue due to several limitations. The first one is related to the fact that the lower the scale, the higher is the internal variability making more difficult the detection of a forced signal from the noise of this variability. The second one is related to the assessment of internal climate variability itself, at the regional scale, that implies requirements that are hardly satisfied. When derived from an observation dataset, the main problem comes from the need to profit by a relatively dense network of observation, over a long time period of at least four to five decades, and qualified through a statistical procedure to correct for heterogeneities. When determined from model simulations, the internal climate variability estimate requires long-range simulations at a spatial scale of the order of a few tenths of kilometers including a representation of coupled air-sea processes. A third limitation comes from the difficulty to evaluate a forced climate change signal due to a poor determination of the forcing at the regional scale (like the aerosol induced radiative forcing) and generally poor ability of large scale climate models to reproduce regional scale features.

The detection of climate change at the regional scale is not a completely new issue. However, according to the synthesis on this subject included in the last IPCC report, 'difficulties remain in attributing temperature changes on smaller than continental scales and over timescales of less than 50 years', and 'attribution at these scales has, with limited exceptions, not yet been established' (Hegerl et al. 2007). As far as the Mediterranean area is concerned, there are very few studies aiming at detecting or attributing formally a climate change signal. We can mention an attempt by Stott et al. (2004) who detected human influence on the temporal pattern of averaged summer temperature over southern Europe, a region close to the Mediterranean area, and Zhang et al. (2006) who detected a spatio-temporal pattern of greenhouse and sulphate aerosol forcing on annual mean temperature over the same region and for the two periods 1900–1949 and 1950–1999. The methodology that is adopted in these two studies is an adaptation of the optimal fingerprint method commonly referred to as the total least squares-based general linear regression of Allen and Stott (2003). This implies that the detection test is not only aimed at rejecting the null hypothesis (the observed variability is only explained by internal climate variability) that is to say the basic detection test, but is also aimed at detecting one or a combination of responses to different forcings in the observations. They are not however attribution studies since all the sources of climate variability were not explored as solar and volcanic forcings. While consistent, the results of the two studies are different since there is no detection for summer temperature in the second one. This is due to the use of different model simulations and, according to the authors of the second mentioned study, to the two different requirements of the

detection analysis, the first one being focused only on a temporal pattern, and the second to a spatio-temporal one. Note that in the case of this second study, the results on the annual mean temperature are even not robust to a doubling of the estimate of internal climate variability.

These two studies are limited to the case of air surface temperature. In the case of precipitation, even at the global scale, only a few studies have investigated the detection or the attribution of changes. Recently, Zhang et al. (2007) have applied the so-called 'optimal fingerprint' detection/attribution methodology to average precipitation within latitudinal bands and concluded that anthropogenic forcing had a detectable influence on observed changes, and that internal climate variability or natural forcing cannot explain these changes. However, to our knowledge, no similar conclusion has been drawn from a detection/attribution study over the Mediterranean area.

The CIRCE project gives a great opportunity to improve as well the dataset, the model simulations and the methodologies that are the basic inputs for detection and attribution studies. At the date of the analyses here reported, a new dataset of homogenized precipitation was available over the Mediterranean domain from Bern University (Kuglitsch et al. 2009), but covering only limited fraction of the area. As far as the methodologies are concerned, new developments have been made in the context of the project in order to improve the ability to detect a climate change signal, possibly of anthropogenic origin, in spite of the above-mentioned limitations. Two of these new methodologies are formal detection procedures in the sense that they consist in applying some statistical test to assess whether observations contain evidence of the expected responses to external forcing that is distinct from variation due to internal climate variability (Hegerl et al. 2007). They have in common the fact that they are aimed at detecting a signal in the spatial distribution of climate change for some climatic parameter (temperature and precipitation in this application). For the so-called 'Regularized Optimal Fingerprint' or ROF method (Ribes et al. 2009), the signal is provided by climate change scenarios for the future. For the so-called 'Temporal Optimal Detection' or TOD method (Ribes et al. 2010), it is inferred from simulations covering the twentieth century. A third methodology, hereafter referred to as 'Consistency' method, focuses on the question whether the recent warming is a plausible harbinger of future warming – that is, we analyze whether the observed changes are consistent with climate change projections. By linking past changes to expected future changes, this analysis helps at providing an illustrative example of what a potential future climate influenced by enhanced greenhouse gas (GHG) concentrations might look like (Barkhordarian et al. 2012; Bhend and von Storch 2008 and 2009).

In the next section we briefly present the observations and modeling outputs that have been used in this study, we then present in Sect. 5.3 the two formal detection methodologies (ROF and TOD) and the 'Consistency' method that have been implemented. A selection of main results obtained by application of the new methodologies to the selected data is given in Sect. 5.4 for temperature and in Sect. 5.5 for precipitation before giving some concluding remarks in the last section.

## 5.2 Data

The domain we have chosen for the Mediterranean area corresponds to the region between 25°N–50°N and 10°W–40°E. This region includes the most commonly defined domains for this area and its boundaries are also chosen in order to match the grid point boundaries of the temperature dataset we have chosen for this analysis. This last is the so-called HadCRUT3v dataset provided by the Climate Research Unit (Brohan et al. 2006). It consists in a combination of monthly values of air temperature anomalies and sea surface temperature anomalies relative to the 1961–1990 period, merged on a 5°×5° grid-box basis and covering the period from 1850 to 2009. This specific version of the dataset results from an adjustment of the grid box average temperature time series for the effects on variance of changing numbers of contributing data through time (Jones et al. 2001). The dataset have been used previously in climate change detection or attribution studies like by Zhang et al. (2006) who applied it to the detection of temperature change over southern Europe (see the introduction). In these applications, the dataset is only used as a reference historical climate dataset, an estimate of internal climate variability, required by the detection or attribution statistical test, being inferred from model simulations. In the present application of the formal detection methods (ROF and TOD), the dataset is also used to estimate internal climate variability as stated in the next section. As the observations include the impact of different forcings, the internal climate variability is then overestimated from the total variability, leading to a more conservative test. The same temperature dataset was also used in the application of the ‘Consistency’ method.

Due to the higher variability of precipitation compared to temperature, this is a greater challenge to obtain good quality dataset to perform detection and attribution studies. Only a few long time series of precipitation covering the twentieth century were available from the CIRCE project for the present analyses. They consist in 17 series of monthly precipitation from Croatian, French and Italian coastal stations, homogenized at Bern University following a methodology presented in Kuglitsch et al. (2009). While some series cover longer periods, the analyses were limited to the period 1900–2004 that is common to all the series. For this dataset, only the ROF and TOD methods were used, considering successively annual, winter and summer averages.

The application of any formal detection method also requires the use of model simulations in order to estimate signals of climate change corresponding to specific forcings. In the present application of the ROF and TOD methods, we focus our analysis on the detection of a spatial pattern of climate change either directly provided from future scenarios simulations or inferred from simulations over the twentieth century (see next section). The simulations are those that are included in the WCRP CMIP3 multi-model dataset archive of the Program for Climate Model Diagnosis and Intercomparison (PCMDI) established at the Lawrence Livermore National Laboratory. Most of these simulations served as the basis for the analyses work synthesized in the fourth IPCC assessment report or AR4 (IPCC 2007).

The present study uses outputs from 24 AOGCMs (Atmosphere Ocean General Circulation Models) that contributed to the CMIP3 simulation exercise. The list of the models can be found on the legend of Fig. 5.2 with a list of acronyms corresponding to those used in the PCMDI database. The models are described on the web portal of this database and, for most of them, in chapter 8 of the AR4. The outputs extracted from these models, correspond to simulations analyzed in the AR4 apart three exceptions. We have not used the outputs of the BCC-CM1 model due to the lack of required fields in the database. We have used the outputs of CSIRO 3.5 and INGV-ECHAM4 AOGCMs included in the CMIP3 database but not in the AR4 list of models.

All the models include the coupling between the atmosphere and the ocean and thus the Mediterranean Sea. Overall, the model horizontal resolutions stand from  $1.4^\circ$  to  $5^\circ$  in the atmosphere and  $0.5^\circ$  (some regions) to  $5^\circ$  in the ocean, with resolutions that are often close to  $3^\circ$  in the atmosphere and  $2^\circ$  in the ocean. The two parameters here considered are the near surface temperature and the precipitation that are provided in the database as monthly horizontal fields. For the application of the ROF method, a scenario of future climate change is required in order to calculate the signal. We have chosen to use the SRES A1B scenario due to its medium range characteristics and the fact that it is available for all the 24 AOGCMs. The choice of different scenarios has not been investigated but previous detection studies with one model and different scenarios have shown that the calculated patterns of climate change are relatively insensitive to the particular scenario as far as temperature is concerned (Ribes et al. 2009). This is mainly due to the fact that, with the proposed methodology, the pattern of the signal can be defined to within a multiplicative factor, and that temperature change between different scenarios are close to be homothetic over the studied region and for a given model. For the application of the TOD method, a simulation covering the twentieth century is required in order to calculate the temporal evolution of the mean temperature over the globe or over the Mediterranean area (see below).

For the application of the ‘Consistency’ method to temperature we have used the outputs from 23 of the CMIP3 global models. A list of the climate models used in this study is given in Table 5.1. The future projections used in this study are based upon the IPCC SRES A1B scenario.

## 5.3 Methods

### 5.3.1 *The “Regularized Optimal Fingerprint”*

This method is more extensively described in Ribes et al. (2009). It is an adaptation of the classical ‘optimal fingerprint method’ introduced by Hasselmann (1993).

As a common framework of presentation of the formal detection methodologies, let assume that an observed climatic parameter at different locations and time steps

is represented by a  $p \times n$  random matrix  $\Psi = (\psi_{i,t})$ . For the present applications  $\psi_{i,t}$  is an observed value either at each point of the HadCRUT3v grid (temperature) or at each of the 17 coastal stations (precipitation) identified by index  $i$ , seasonally or annually averaged (possibly over a 30-year period for the application) at a given time identified by index  $t$ . This observed parameter is assumed to be represented as a superposition of a deterministic climate change signal  $\psi_{i,t}^S$  and one random realization of internal climate variability  $\tilde{\psi}_{i,t}$ :

$$\psi_{i,t} = \psi_{i,t}^S + \tilde{\psi}_{i,t} \quad (5.1)$$

For the sake of simplicity of the presentation, without any loss of generality, we will assume that  $\tilde{\psi}_{i,t}$  is centered i.e.  $E(\tilde{\psi}_{i,t}) = 0$  where  $E()$  stands for the expectation.

An additional hypothesis is also made in the present application assuming that the internal climate variability has the structure of an AR1 process for temperature or that the  $(\tilde{\psi}_{i,t})$  are independent identically distributed random variables for precipitation. The difference in the treatment of temperature and precipitation accounts for the fact that temperatures are more correlated with time than precipitation. The AR1 process was adjusted using the outputs of a few control climate simulations from the CMIP3 database.

It is also assumed that the spatial pattern of climate change is given to within a multiplying factor function of time, equivalent to a time-space separation assumption:

$$\psi_{i,t}^S = \mu_t g_i \quad (5.2)$$

where the  $\mu$  vector of dimension  $n$  is the temporal pattern and the  $g$  vector of dimension  $p$  is the spatial pattern.

The detection process consists in testing the  $H_0$  hypothesis saying that the observation matrix  $\Psi$  is derived from internal climate variability statistics versus the  $H_1$  hypothesis saying that some climate change signal is added to this internal climate variability.

For the ROF method, similarly to the classical adaptation of optimal fingerprint, the  $g$  vector is supposed to be known and derived from future scenarios simulations as a guess-pattern. The detection test thus reduces to the test at each time step of the null hypothesis  $H_0$ :  $\mu_t = 0$  versus the  $H_1$  hypothesis:  $\mu_t > 0$ .

Following Hasselmann (1993), the null hypothesis is tested at each time step in a direction that maximizes the signal to noise ratio resulting in applying the test to a detection variable given by:

$$d_j = f^T \psi; \quad \text{with: } f = C^{-1} g \quad (5.3)$$

where  $f$  is the so-called 'fingerprint' and  $C$  the spatial covariance matrix of the internal climate variability.

In the ROF adaptation of the 'optimal fingerprint' method,  $C$  that is unknown is replaced by  $\hat{C}_t = \gamma \hat{C} + \rho I$ , where  $\hat{C}$  is the 'classical' empirical estimate of  $C$ ,  $I$  is the identity matrix and the coefficients  $\gamma$  and  $\rho$  are chosen in order to obtain a good

estimate of  $C$ . Compared to the common application of the ‘optimal fingerprint’ method, this calculation leads to a more powerful statistical test, and has the advantage to avoid the inversion of  $\hat{C}$  in a space of reduced dimension. A bootstrap technique is used in order to determine the threshold of rejection of the null hypothesis and the p-values (the probability to exceed the value of the detection variable given the null hypothesis is true) (Ribes et al. 2009).

In the present application, the detection study applies to moving averages of annual or seasonal temperature and precipitation over 30-year periods, calculated either at each point of the HadCRUT3v grid (temperature) or at each of the 17 coastal stations (precipitation). The temperature and precipitation are either those directly observed or are spatially centered values after the removal of the spatial average over all the observed series at each time.

The spatial guess-pattern of climate change  $g$  is, as stated before, calculated from CMIP3 climate change simulations corresponding to the SRES A1B scenario. It is obtained, at each model grid point in the domain, as the difference between the simulated mean temperatures of a 30-year period at the end of twenty-first century and the simulated mean temperature of the 1960–1989 period. For each of the AOGCMs, the pattern is interpolated at the location of the HadCRUT3v grid (temperature) or of the 17 stations (precipitation) using a conservative interpolation procedure.

In addition to the detailed algorithm presented in Ribes et al. (2009), a pre-whitening technique is used in order to account for an AR1 time-dependent structure of the temperature data.

### 5.3.2 The “Temporal Optimal Detection”

The TOD method is more extensively described in Ribes et al. (2010). The common hypotheses with the ROF method and its application to the present case are the following:

- The observed parameters are a superposition of a deterministic climate change signal and one random realization of internal climate variability (Eq. (5.1)).
- The signal is determined through a time-space separation assumption given in Eq. (5.2).
- The internal climate variability has the structure of an AR1 process for temperature or the  $(\tilde{\Psi}_{i,t})$  are supposed to be independent identically distributed random variables for precipitation.

Contrary to the ROF and the classical “optimal fingerprint” method, the  $g$  vector is not supposed to be known while the  $\mu$  vector is supposed to be known. The detection test thus reduces to the test of the null hypothesis  $H_0: g = 0$  versus  $H_1$  hypothesis:  $g \neq 0$ .

The first step of the method consists in determining the  $\mu$  vector. By symmetry with the ROF method, it is obtained from model simulations that account for the

anthropogenic forcing but over the twentieth century rather than for future conditions. This pattern should reflect the temporal evolution of the expected climate change signal, whatever the index that is used to determine this climate change. As the climate change signal is more clearly identified on temperature, the bases of the calculation are spatially averaged temperature over the globe, inferred at each time step of the observing period from each AOGCM simulation. We also constrain this estimate to be rather smooth over the observing period used for the detection test following the procedure described in Ribes et al. (2010).

The second step of the method is the application of the detection statistical test. It can be shown that, with the current hypotheses, the detection test reduces to the so-called Hotelling test. This test provides an estimate of  $g$  and the associated p-value of the test.

In the present application of the method, as for the application of the ROF method, the detection study applies to the observed series of annual or seasonal mean temperature and precipitation calculated either at each point of the HadCRUT3v grid (temperature) or at each of the 17 costal stations (precipitation). As for the application of the ROF method, the temperature and precipitation are either those directly observed or spatially centered values after the removal of the spatial average over all the observed series at each time.

### 5.3.3 *The 'Consistency' Method*

In this study, we link past and future changes using a set of hierarchical questions.

First, we analyze whether external influences on the observed change are detectable. Therefore, we compare the observed change with estimates of the natural variability (i.e. internal variability and variability due to other unaccounted factors) derived from the observed record with a bootstrap procedure. We further compare the observed change to estimates of internal variability derived from the control runs of CMIP3 climate models (Sect. 5.2).

Second, we analyze if the combination of GHG and sulfate forcings (GS forcing) is a plausible explanation for the observed change, taking into account, that both internal variability and other external (but unspecified) forcings influence the observed record.

The analysis as described above is carried out for each of the models individually. The last step of the analysis, in contrast, is an overall assessment. We consider the 23 climate change projections according to the SRES A1B scenario and determine whether the recent trend is within this range of expected change due to GS forcing, and could thus be seen as a harbinger of future change.

Consistency with projections – as defined above – does not demonstrate cause and effect relationships; these would require a formal attribution study (that we are unable to provide at the moment as we consider the understanding of many of the important forcing mechanisms at the regional scale as insufficient). Consistency, in contrast, points to the plausibility (not probability) that the recent trend will con-

tinue into the future – based on the understanding that the recent trend is related to the known forcing, which will continue into the future. Thus, our assessment aims at providing an illustrative example of a potential future by comparing the observed change to one hypothetically dominant forcing, GS forcing in this case (Bhend and von Storch 2008, 2009; Barkhordarian et al. 2012).

Trends in observations have been calculated using ordinary least squares linear regression. We define the anthropogenic climate change signal as the difference between the last decades of the twenty-first century (2071–2100) and the reference climatology (1961–1990). We assume a linear development from 1961 to 2100 and the resulting signal is scaled to change per decade. Using well-separated time slices, 110 years in this study, has the advantage of increasing the signal-to-noise ratio and there is no need to average multiple models to get good signal estimates. Thus, this allows us to investigate the robustness of our results to using different climate models and to explicitly deal with individual models separately.

Additional analyses show that by assuming a constant warming rate, we slightly overestimate the actual rate of warming from 1979 to 2009. We found no evidence of a discernible change in the pattern of warming during the period from 1961 to 2100 (Barkhordarian et al. 2012). The advantage of a much higher signal-to-noise ratio of an anthropogenic signal when estimated from time slices justifies the use of time-invariant warming patterns as opposed to transient warming patterns.

The comparison of observed and anthropogenic climate change signal patterns are carried out using three pattern similarity statistics. We use both centered and un-centered pattern correlation (Eqs. (5.4) and (5.5) respectively). The un-centered correlation ( $UC$ ) measures the similarity of two patterns without removal of the spatial mean, while the centered correlation ( $CC$ ) refers to the correlation of deviation patterns, where the spatial mean has been subtracted (Santer et al. 1993). The third pattern similarity statistics is regression (Eq. (5.6)). Unlike the correlation statistics, this measure ( $F$ ) includes information about the relative magnitudes of the observed and model projected trend patterns.

$$UC(O, P) = \frac{\sum_{i=1}^n P_i Q_i}{\sqrt{\sum_{i=1}^n P_i^2 \sum_{i=1}^n Q_i^2}} \quad (5.4)$$

$$CC(O, P) = \frac{\sum_{i=1}^n (P_i - \bar{P})(Q_i - \bar{Q})}{\sqrt{\sum_{i=1}^n (P_i - \bar{P})^2 \sum_{i=1}^n (Q_i - \bar{Q})^2}} \quad (5.5)$$

$$F(O, P) = \frac{\sum_{i=1}^n P_i Q_i}{\sum_{i=1}^n P_i^2} \quad (5.6)$$

The index subscript  $i = 1, \dots, n$  counts the spatial points.  $Q_i$  and  $P_i$  refer to the observed and expected pattern of change, respectively.

The un-centered correlation and regression statistics combine both spatial-mean and pattern information. In order to have a measure without the effect of spatial

pattern information, we also compare the area-mean changes of observed and anthropogenic signal patterns.

To evaluate the significance of pattern similarity statistics, we use a bootstrap technique to test the null hypothesis that the observed trends are drawn from an undisturbed stationary climate (von Storch and Zwiers 1999). Thus, we separate between GS-related change and “non-GS” variability. This “non-GS” variability includes all natural factors, which are assumed to remain stationary in the coming century, i.e. not only internal variability but also other unaccounted external factors, such as volcanoes, solar and aerosol forcings. We estimate “non-GS” variability by re-sampling the observational record using a moving block bootstrap technique (Wilks 1997). The block length chosen for the moving blocks bootstrapping depends on the autocorrelation of the seasonal temperature time series. This is different for different grid boxes and different seasons. Our analysis based on a method suggested by Wilks (1997), indicates that the average block length across the Mediterranean is 2.2, 3.5, 5, and 2.8 for DJF, MAM, JJA and SON, respectively. We choose a block length of five that should lead to slightly conservative confidence intervals at most grid boxes. We draw 1,000 30-year time series to estimate the variability of 30-year trends in a stationary climate. Furthermore, we use the bootstrapped trend patterns to disturb the observed trend patterns and then compute the same pattern similarity statistics. By doing so, we sample the range of non-GS variability in the observed trends. Quantiles of these bootstrapped pattern similarity statistics are then used to describe the non-GS-variability of the pattern similarity statistics. Of course, question remain as to what extent the time series length (160 years in this study) is sufficiently long for giving reliable estimates of variability.

In the present application of the method, trends in observations have been calculated using ordinary least squares linear regression applied to the HadCRUT3v dataset. We do not compute trends for grid boxes with more than 6 years of missing values. We compare near-surface temperature trends over land and sea for the period from 1979 to 2009 with climate change projections derived from the CMIP3 climate simulations. We analyze both annual and seasonal average change and pattern similarity.

## 5.4 Temperature Change

### 5.4.1 Formal Detection

We have reported in Fig. 5.1 the map of the HadCRUT3v grid point taken into account for the formal detection study. Both ROF and TOD method cannot be applied with missing data. Over the 1900–2009 period, 21 grid points have no missing data. In order to increase the number of grid points with no missing data, we choose to remove some years from the initial dataset. An optimal balance was found while removing 9 years from the 1900 to 2009 period (mainly during world wars), and adding 8 grid points to the 21 complete time series.

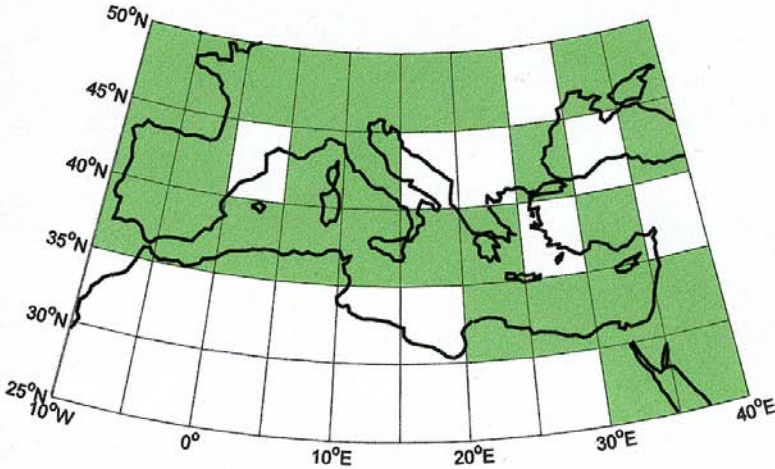


**Fig. 5.1** Data coverage; the *green* colored meshes show no missing data after having removed 9 years from the 1900 to 2009 period; these grid points are taken into account in the formal detection studies

The formal detection studies are then based on 29 grid points over the Mediterranean area, leading to a proper coverage, except over the continental North Africa.

#### 5.4.1.1 Annual Mean

We first present the results of the application of the ROF method to the 30-year moving averages of the annual mean temperatures calculated over the Mediterranean area (Fig. 5.2 top). For each of the 30-year period, the detection variable of the ROF method is calculated with an equation similar to Eq. (5.3). In this equation, the observation vector and the estimate of the inverse of the spatial covariance matrix of the internal climate variability, come from the HadCRUT3v dataset, and the spatial guess-pattern come from the climate change signal simulated by each of the 24 AOGCMs of the CMIP3-PCMDI database. In Fig. 5.2, the p-values of the ROF detection test are presented on a neperian logarithmic scale with an indication of the 5% significance level. We can see that, at the end of the period, a climate change signal is detected at the 5% significance level with all of the AOGCMs spatial guess-patterns. This result is consistent with the finding of Zhang et al. (2006) obtained with a different formal detection method over a slightly different domain (southern Europe). The dispersion of the models is increasing with time, that is partly an artifact of the logarithmic representation that inflates the differences for lower p-values.

When considering the spatially centered temperatures (after the removal, at each time, of the spatial averages over the domain, applied to the observed fields and the spatial guess-patterns), the detection is still successful for many AOGCMs (Fig. 5.2 bottom). The 5% significance level of the detection is reached for 20 AOGCMs over, at least, some years of the last decade. Very low p-values are obtained with some

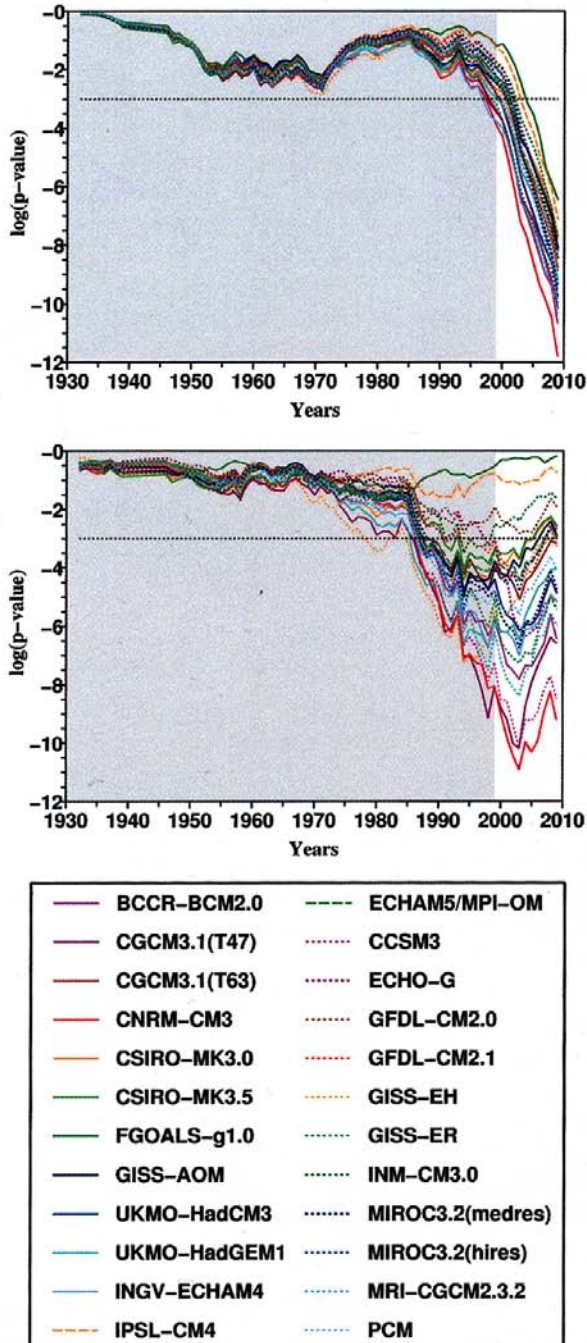


**Fig. 5.2** Detection of annual mean temperature change (*top*) and of spatially centered annual mean temperature change (*bottom*) over the Mediterranean area with the ROF method. The p-values of the ROF detection statistical test are presented in neperian logarithmic scale for each of 24 AOGCMs with their acronyms as appearing in the CMIP3-PCMDI database. The simulations

AOGCMs, and the detection occurs sooner than in the previous case with many patterns. It is worth noting that the detection test is here much more challenging since we only keep the spatially varying part of the observed and estimated signal fields. This result shows that the whole climate change signal is not provided by the global warming alone.

We then present the results of the application of the TOD method to periods of time of varying lengths, all starting in 1900 and ending between 1920 and 2009. As a first step of the method, the temporal guess-pattern needs to be inferred from AOGCMs simulations (see Sect. 5.2). We show in Fig. 5.3 (top) the results of the adjustment over the 1900–2009 period and each of the AOGCMs, using the globally averaged annual mean temperatures, and 4 equivalent degrees of freedom. The patterns show an increasing temperature over the period but the shape of the curves are varying from a quasi linear evolution to a quadratic-like behavior, with even a decrease followed by an increase. Such discrepancies are partly explained by the different external forcings taken into account by the many AOGCMs over the twentieth century. In particular, the separation between AOGCMs that simulate only anthropic forcings and the ones accounting for all forcings is done in Fig. 5.3. When the mean averages are calculated over the Mediterranean domain with the same smoothing parameters (Fig. 5.3 bottom), the patterns show the same kind of variability and, for each specific model, the regional temporal pattern generally resembles the global one.

As a second step of the TOD method, the Hotelling test is applied to the multivariate regression model (8) where the observations are the HadCRUT3v spatially centered annual mean temperatures over the Mediterranean area and the temporal guess-patterns are either adjusted from global means of simulated temperatures (Fig. 5.4 top) or from regional means of simulated temperatures over the Mediterranean area (Fig. 5.4 bottom). The p-values of the TOD detection test are presented on a neperian logarithmic scale with an indication of the 5% significance level. We can see in Fig. 5.4 (top) that the 5% significance level of the detection is reached by all the AOGCMs for virtually all the periods that are longer than the period 1900–1965. For most of the AOGCMs, the detection with the regional temporal pattern (Fig. 5.4 bottom) is only marginally delayed, confirming the visual similarity of the temporal patterns (Fig. 5.3). The dispersion of the p-values is also somewhat increased, similarly to the dispersion of the guess patterns. The models that give the largest p-values are those that simulate a cooling at the beginning of twentieth century.

Compared to the ROF detection test (Fig. 5.2), the detection of a climate change signal appears more clearly. This can be associated to the fact that the TOD method requires less constraints from models since they only provide a smoothed temporal guess-pattern and not the spatial distribution of the climate change signal. This last

←  
**Fig. 5.2** (continued) associated to a *solid line* include only anthropogenic forcing and those associated to a *dotted line* also include natural forcings (solar and volcanic). The value for 1 year period corresponds to the treatment of HadCRUT3v annual mean temperatures averaged over a 30-year period ending this specific year; the hatched *horizontal line* corresponds to a p-value of 0.05 implying a 5% significance level of the detection (see text for the details). The *grey background* shows the period where the learning sample (for estimating the covariance matrix) and the tested average are not completely separated

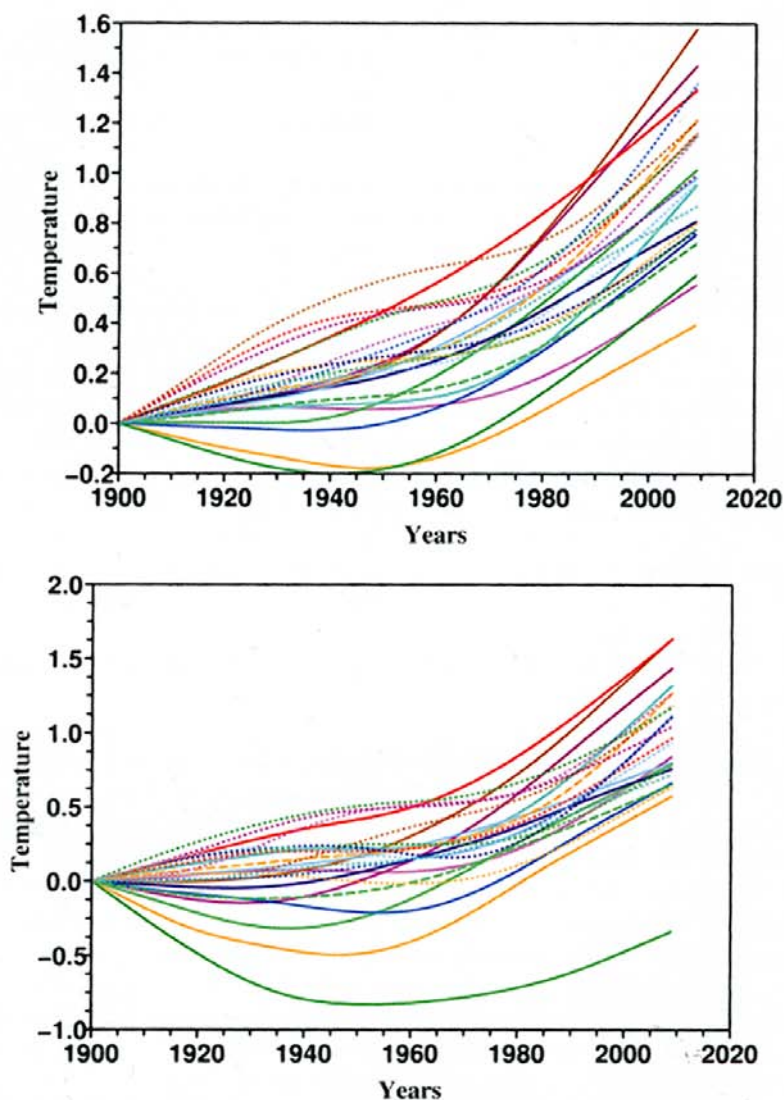


**Fig. 5.3** Temporal guess-patterns adjusted from the global mean temperatures (*top*), and from the regional averages of temperature over the Mediterranean area (*bottom*), simulated by 24 AOGCMs. The period of adjustment is 1900–2009 and the smoothing parameter is the same for all the models (see text for the details). Legend as in Fig. 5.2

is on the contrary a product of the detection process (see Sect. 5.3.2) that is illustrated in Fig. 5.5 for the detection applied with the temporal guess-patterns of regional mean temperature over the Mediterranean area.

The reproduced map is the ensemble average of the spatial patterns of annual mean temperature change, that results from the application of the TOD method

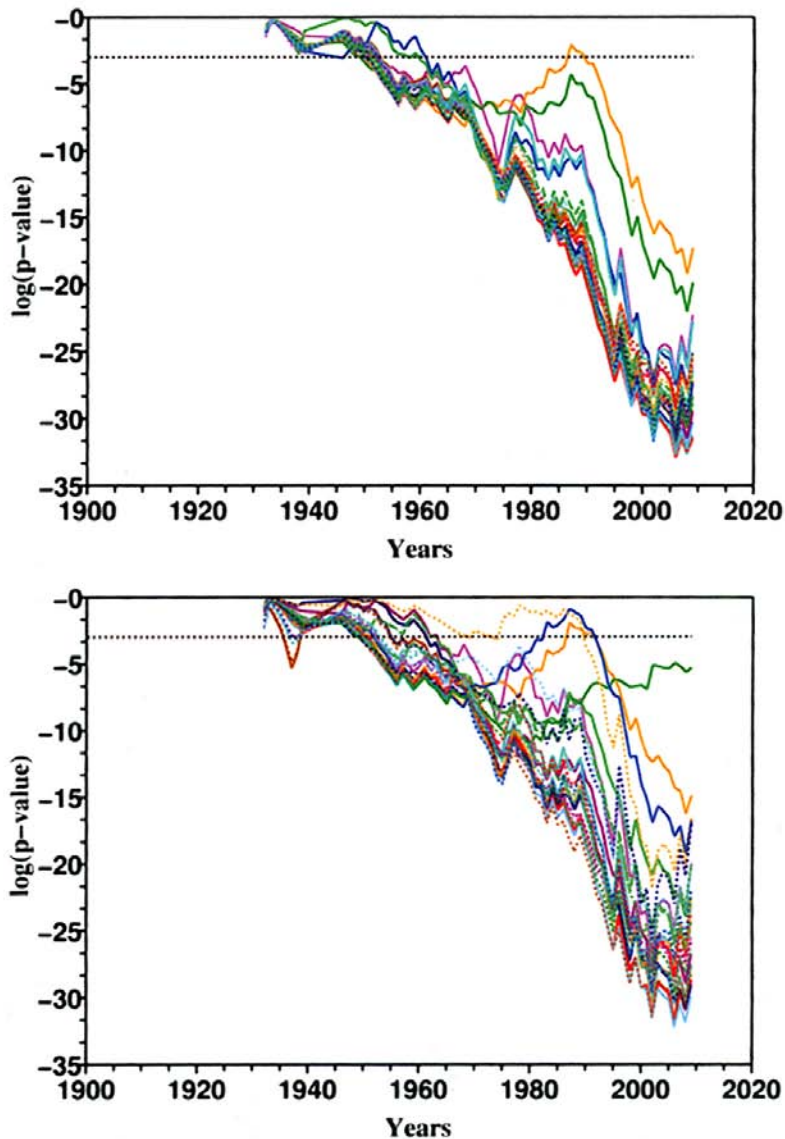


**Fig. 5.4** Detection of spatially centered annual mean temperature change over the Mediterranean area with the TOD method using temporal guess-patterns of global mean temperature (*top*) and regional mean temperature (*bottom*). The guess patterns are adjusted from the global mean temperatures simulated by 24 AOGCMs. The p-values of the TOD detection statistical test are presented in neperian logarithmic scale for each AOGCM; the value for 1 year corresponds to the treatment of HadCRUT3v annual mean temperatures over a period starting at 1900 and ending this specific year; the hatched horizontal line corresponds to a p-value of 0.05 implying a 5% significance level of the detection (see text for the details). Legend as in Fig. 5.2

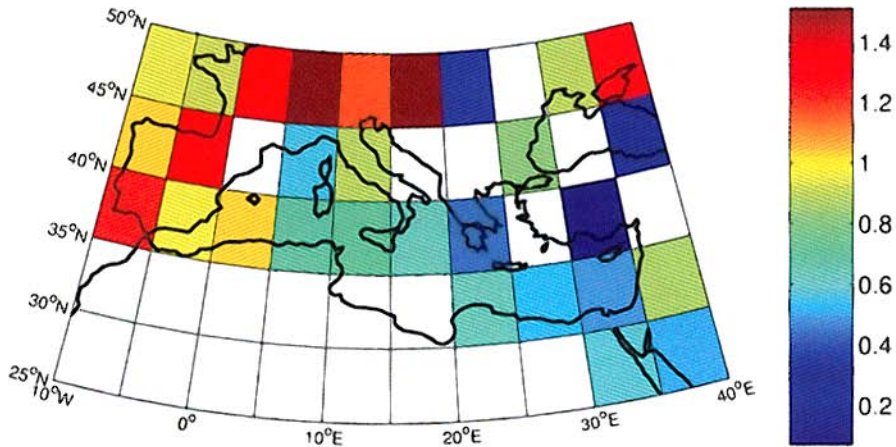


**Fig. 5.5** Spatial pattern of annual mean temperature inferred from the TOD method using temporal guess-patterns of regional mean temperature (see Sect. 5.3.2); the method is here applied over the 1900–2009 period and the regional guess patterns are adjusted from the regional mean temperatures simulated by 23 AOGCMs: this map is an average for the whole AOGCMs ensemble

using the temporal guess-patterns of 23 different AOGCMs (the FGOALS model is not considered in the ensemble due to its atypical regional temporal guess-pattern). In this case, the minimum spatial correlation coefficient between two different spatial patterns, calculated from all the couples of AOGCMs of the ensemble, is equal to 0.93. This points out the great consistency between the different retrievals implied by the relative resemblance of the temporal patterns shown in Fig. 5.3 (bottom). This consistency occurs while the models reproduce differently internal climate variability and include, for only some of them, natural forcings (solar and volcanic). This implies that the pattern reflects more or less the anthropogenic part of the climate change signal or that the signals of different origins cannot be clearly distinguished. The temporal pattern increasing and being positive for the most part of the models and periods, the inferred spatial pattern shows a greater warming for the north-western part of the domain compared to the eastern part.

#### 5.4.1.2 Seasonal Means

We present in this section some results obtained from the application of the TOD and ROF detection methods to winter (December–January–February) and summer (June–July–August). We limit this presentation to the case of the detection of spatially centered seasonal mean temperature change over the Mediterranean area with the TOD method using temporal guess-patterns of regional mean temperature and with the ROF method.

In winter (Fig. 5.6 top), with the TOD method, the detection reaches the 5% significance level for the most part of the AOGCMs (17) for all the periods that are longer than the period 1900–1980 that is to say later than for the annual mean. For

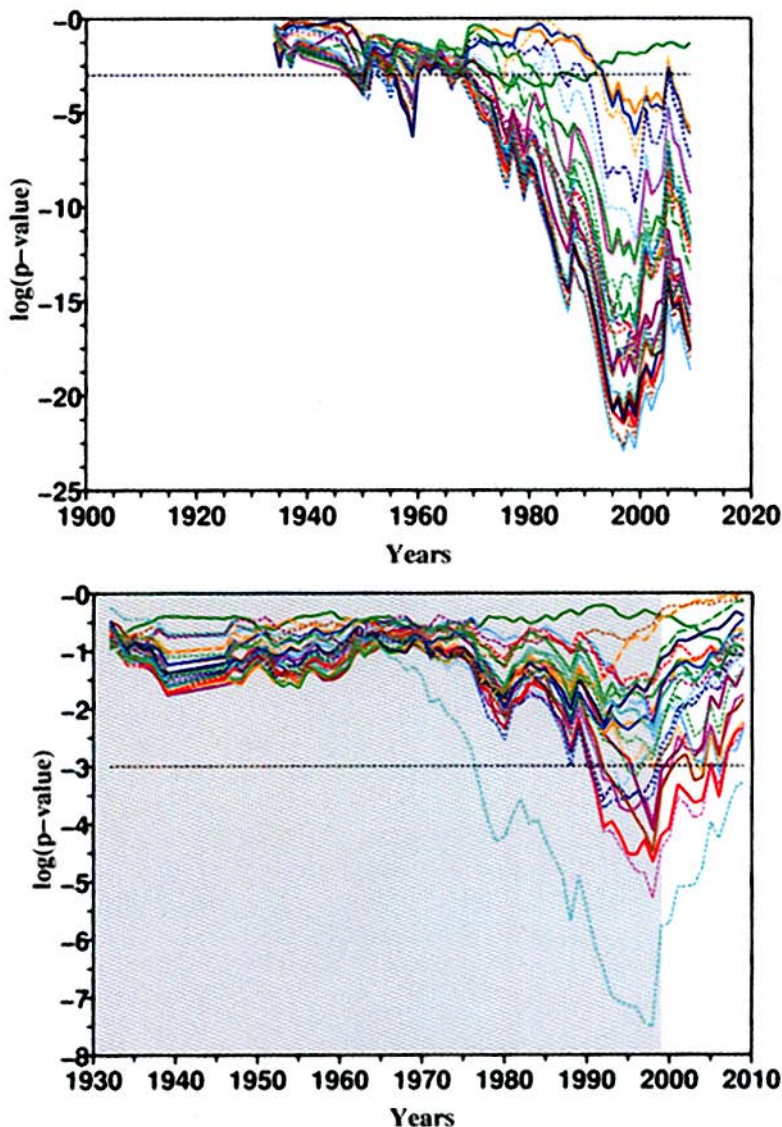


**Fig. 5.6** Detection of spatially centered winter mean temperature change over the Mediterranean area with the TOD method using temporal guess-patterns of regional mean temperature (*top*) and with the ROF method (*bottom*). Same graphic conventions than in Fig. 5.4 (*bottom*) and Fig. 5.2 (*bottom*) respectively. Legend as in Fig. 5.2

the longest periods, the p-values of the detection is increasing suggesting a possible contamination of the climate change signal with low frequency variability that could be of internal origin. Further investigation is needed in order to evaluate potential impact of the change in frequency of climate regimes. However, we can conclude

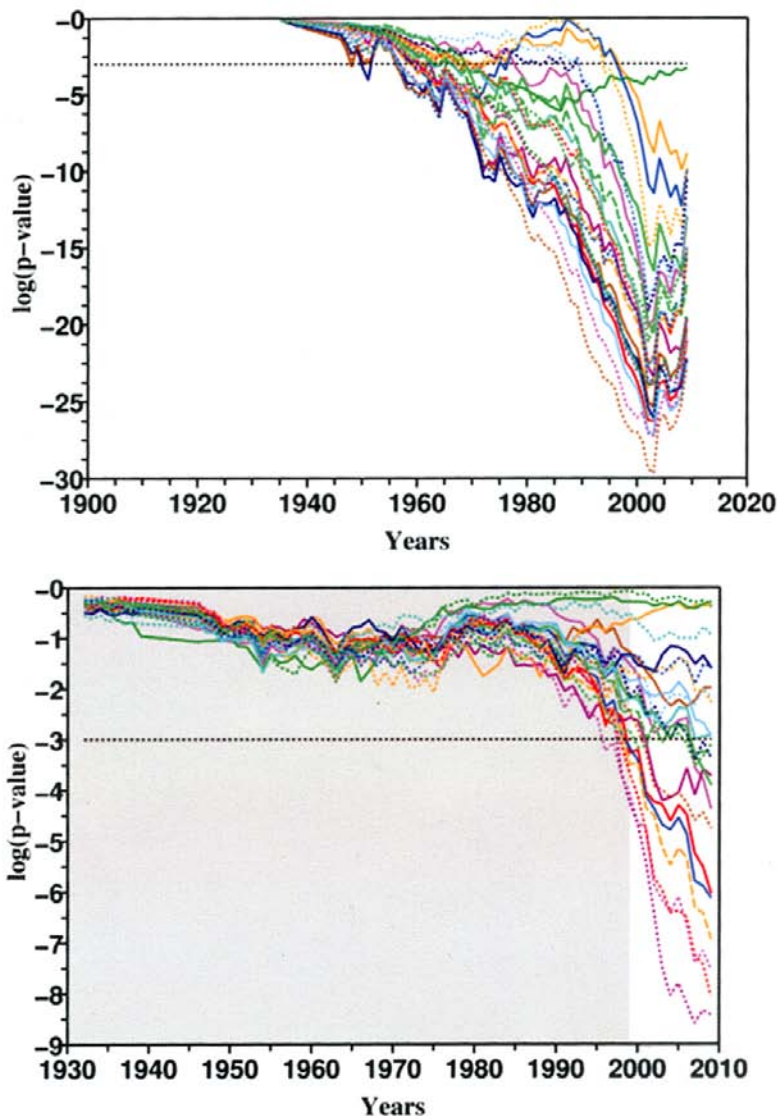


**Fig. 5.7** Detection of spatially centered summer mean temperature change over the Mediterranean area with the TOD method using temporal guess-patterns of regional mean temperature (*top*) and with the ROF method (*bottom*). Same graphic conventions than in Fig. 5.4. (*bottom*) and Fig. 5.2 (*bottom*) respectively. Legend as in Fig. 5.2

from this graph that the null hypothesis can be rejected with a high level of significance, even when including the most recent years. The same kind of behavior can be seen with the application of the ROF method but with only a few AOGCMs giving a 5% significance level for the detection (Fig. 5.6 bottom). This ensemble of result extends the conclusions of previous studies concerning southern Europe.

In summer, with the TOD method, with the same exception than for winter, almost all the AOGCMs temporal guess-patterns allow to reject the null hypothesis at the 5% significance level when including the observations of the last decades (Fig. 5.7 top). The detection occurs sooner than in winter and the p-values are mainly decreasing when extending the period (except over the very last years). With the ROF method, the detection at the 5% significance level here is also reached for roughly a half of the AOGCMs at the end of the period (Fig. 5.7 bottom).

This ensemble of results confirms the previous analysis of Stott et al. (2004) applied nearly to the same region since the domain of the two studies only differ by 5° at their southern boundaries. Moreover, it also extends it because we have used a wider ensemble of simulations and, moreover, because the present detection applies to spatial patterns of climate change, after spatial centering of the data.

## 5.4.2 Consistency Analysis

As detailed in Sect. 5.3.3, the ‘Consistency’ analysis is a three-step process.

### 5.4.2.1 Is the Observed Warming Due to Natural (Internal) Variability Alone?

The comparison of observed area mean change of seasonal near-surface temperature over the period from 1979 to 2009 and the multi-model ensemble mean response (a mean over all available ensemble members) is shown in Fig. 5.8. The observed warming is likely not due to natural variability (non-GS variability) alone in cases where the 90% uncertainty range (black bars in Fig. 5.8) derived from bootstrapped trends excludes zero. As shown in Fig. 5.8, externally forced changes are detected in the observed annual area-mean warming and in all seasons except winter (with a probability of error of less than 5%).

To investigate the robustness of our results to using model-based internal variability, we compare the observationally based estimate of internal variability with the variability estimated from the control runs, derived from the 23 models used in this study. Our results show that in all seasons, the variability based on the control runs of the 23 models is smaller than the variability estimated from block bootstrapping, indicating that the detection of externally forced changes in the observed trends over the Mediterranean is robust to using model-based estimate of internal variability.

We are also able to detect an external influence using different pattern similarity statistics. Table 5.1 shows the seasonal and annual un-centered pattern correlation coefficients of observed near-surface trends from 1979 to 2009 with anthropogenic signals derived from the 23 models in the CMIP3 archive. The annual un-centered correlation coefficients are in the range of 0.91–0.97 and these correlations are larger than the 95% quantiles of bootstrapped pattern correlations. In summer (JJA)

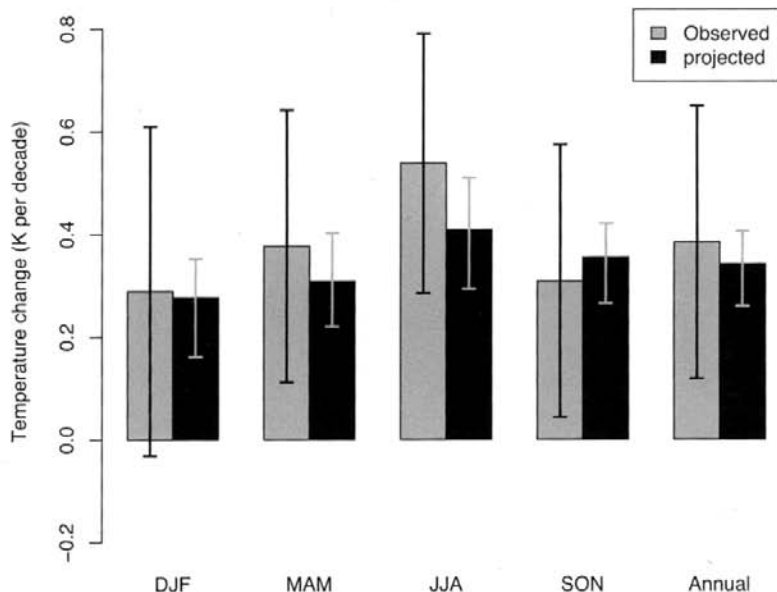


**Fig. 5.8** Observed seasonal and annual area mean changes of near surface temperature over the period 1979–2009 in comparison with anthropogenic signals (GS) according to the SRES A1B scenario derived from the CMIP3 multi-model ensemble mean. From *left to right* winter, spring, summer, autumn and annual. The *grey* whiskers indicate the spread of trends of 23 climate change projections used in this study. The *black* whiskers denote the bootstrap 90% confidence interval of observed trends

all climate change projections share very high un-centered correlation coefficients ranging from 0.92 to 0.97 which are significant at the 2.5% level.

The correlation of observed trend patterns with anthropogenic signal patterns is also high in spring (MAM) and autumn (SON). In spring, the coefficients are ranging from 0.87 to 0.93 (significant at 2.5% level) and in autumn from 0.85 to 0.90 (significant at 2.5% level). Indeed such correspondence can hardly (less than 2.5% level) be expected to show up if only “non-GS” forcing would be present. Although, we do not find a detectable external influence using centered pattern correlation (not shown), in which the spatial-mean is removed and the pattern is simply a spatial anomaly pattern.

When using regression as a pattern similarity measure, which unlike the correlation statistics measures the relative magnitude of the observed and model projected trend patterns, we are able to detect external influences in annual warming and in all seasons except in winter. Figure 5.9 displays the regression coefficients and their 95% confidence interval. Detection of GS signal is claimed at 2.5% significant level when the uncertainty range does not include zero. As shown in Fig. 5.9 in spring, summer and autumn the uncertainty interval does not include the zero line in all cases. Therefore, we conclude that there is less than a 2.5%

**Table 5.1** Seasonal and annual un-centered pattern correlation coefficients of near-surface temperature for 30-year trends from 1979 to 2009, compared to the trend of 23 anthropogenic climate change scenarios derived from the CMIP3 multi-model data set

Models	DJF	MAM	JJA	SON	Annual
BCCR-BCM2.0	0.88	0.92*	0.96*	0.87*	0.95*
CCCMA-CGCM3.1(T47)	0.87	0.90*	0.91*	0.87*	0.93*
CCCMA-CGCM3.1(T63)	0.86	0.93*	0.92*	0.86*	0.93*
CNRM-CM3	0.88	0.87*	0.97*	0.88*	0.95*
CSIRO-MK3.0	0.82	0.87*	0.94*	0.89*	0.95*
CSIRO-MK3.5	0.89	0.87*	0.96*	0.89*	0.95*
GFDL-CM2.0	0.88	0.90*	0.96*	0.87*	0.95*
GFDL-CM2.1	0.89	0.87*	0.96*	0.87*	0.92*
GISS-AOM	0.87	0.88*	0.94*	0.88*	0.94*
GISS-EH	0.85	0.84*	0.94*	0.88*	0.95*
GISS-ER	0.88	0.84*	0.92*	0.85*	0.92*
INGV-ECHAM4	0.88	0.90*	0.94*	0.85*	0.94*
INM-CM3.0	0.87	0.87*	0.96*	0.89*	0.95*
IPSL-CM4	0.88	0.90*	0.96*	0.88*	0.95*
MIROC3.2(hires)	0.88	0.88*	0.97*	0.88*	0.97*
MIROC3.2(medres)	0.87	0.90*	0.96*	0.89*	0.96*
MIUB-ECHO-G	0.89	0.93*	0.96*	0.87*	0.93*
ECHAM5/MPI-OM	0.88	0.88*	0.96*	0.88*	0.94*
MRI-CGCM2.3.2A	0.87	0.91*	0.96*	0.87*	0.95*
NCAR-CCSM3-0	0.89	0.92*	0.96*	0.88*	0.94*
NCAR-PCM1	0.89	0.89*	0.94*	0.89*	0.96*
UKMO-HadCM3	0.88	0.90*	0.97*	0.87*	0.95*
UKMO-HadGEM1	0.87	0.92*	0.97*	0.89*	0.95*

The indices significantly greater than zero at 2.5% level are labeled with an asterisk

chance that natural (internal) variability rather than the GS signal is responsible for the observed change.

Significant un-centered correlation coefficients and regression indices clearly indicate that the combined large-scale (spatial mean) and small-scale (anomalies about the mean) component of GS signal is detected in annual mean warming and all seasons except in winter. Failure to detect the smaller-scale component (spatial anomalies about the mean) of GS signal in observed trend patterns indicates that the spatial-mean is the important and dominant component of the GS signal. We have to be aware, however, that both spatial coverage and representativeness of the observations as well as potential model errors at grid-box-scale have a strong influence on the similarity of spatial anomaly patterns.

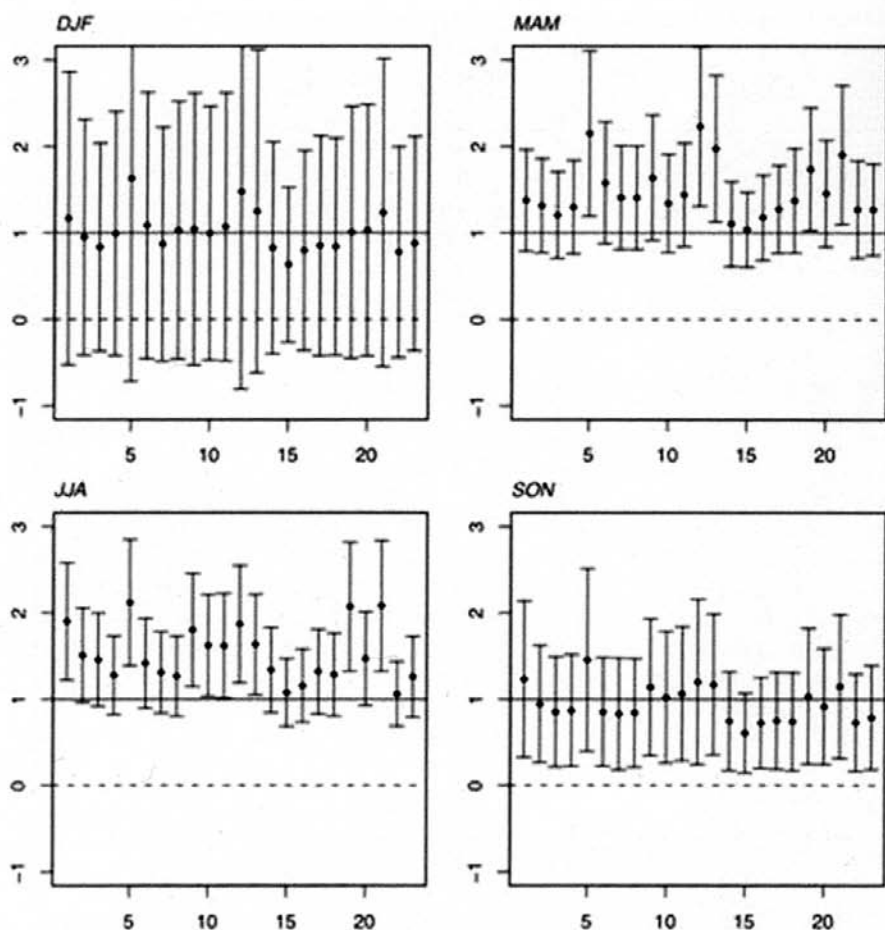


**Fig. 5.9** Regression coefficients of observed near-surface temperature changes against simulated in response to GS forcing according to the SRES A1B scenario derived from 23 models. The bars show the 95% uncertainty ranges of regression coefficients derived from the observed record using a moving blocks bootstrap. The solid horizontal lines mark regression indices equal to unit scaling indicating consistency with GS forcing

#### 5.4.2.2 Is GS-Forcing a Plausible Explanation of the Observed Warming?

We investigate whether GS-forcing is a plausible explanation of the observed warming, given that the observed warming is further subject to internal variability and influenced by other external forcings. For seasonal and annual area-average warming in Fig. 5.8, we find that all model-derived GS signals (grey bars) lie within the uncertainty bound about the observed change indicating the influence of non-GS variability (black bars). From this we conclude that GS-forcing is consistent with the observed warming.

These results are further confirmed when taking the spatial pattern of change into account. Figure 5.9 displays the regression coefficients and its 95% confidence interval. The observed change is consistent with GS forcing if the uncertainty range of regression coefficients includes unit scaling. The observed annual area-mean warming is not significantly different from projections as unit scaling of all 23 projections is well within the uncertainty bars (see Table 2 in Barkhordarian et al. 2012), this suggests that the hypothesized forcing, GS, is a plausible explanation of the observed annual area-mean warming, with a probability of error less than 2.5%.

In spring, the regression coefficient of the observed change on GS signals from individual models is not significantly (at 2.5% level) different from unit scaling with 18 out of 23 models. In summer, the uncertainty ranges on regression coefficients include unity with 16 out of the 23 models. This suggests that in summer and spring some of the models significantly underestimate the amplitude of observed warming. In autumn, the uncertainty range of regression indices includes unity in all cases. Thus, we find consistency with all of the 23 models in autumn.

#### **5.4.2.3 Is the Observed Change a Plausible Illustration of Future Expected Changes?**

In this section, we analyze whether the observed warming in the Mediterranean is indistinguishable from the range of CMIP3 projections – i.e. whether the CMIP3 projections encompass the observed warming. If this is the case, we conclude that the observed warming serves as a plausible illustration of future change to be expected in this region.

When analyzing area-average warming (Fig. 5.8), we find that the projections encompass the observed warming in all seasons except in summer. Thus we conclude that the observed area-average warming can be used to illustrate the future expected warming in the Mediterranean except in summer.

When taking into account the spatial pattern of the change as well, we find that regression estimates encompass unit scaling only in all seasons. However, in spring and summer, most of the projections underestimate the observed warming thus resulting in regression coefficients larger than one (see Barkhordarian et al. 2012 for further details). These results together with the low centered correlation coefficients point to the fact, that the spatial features of the observed warming do not well represent the expected future warming due to GS forcing.

## **5.5 Precipitation Change**

The application of the ROF method requires the use of the AOGCMs spatial guess-patterns. Due to the high spatial variability of the precipitation field and the challenge of its modeling, the detection of a climate signal using this methods appears to be a greater challenge than the application of the TOD method that only requires

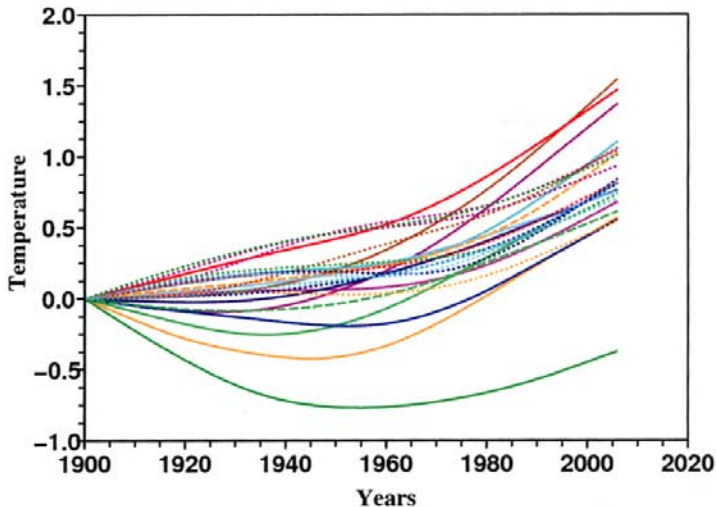


**Fig. 5.10** Temporal guess-patterns of regional averages of temperature over the Mediterranean area; the guess patterns are adjusted from the global mean temperatures simulated by 24 AOGCMs with their acronyms as appearing in the CMIP3-PCMDI database; the period of adjustment is 1900–2004 and the smoothing parameter is the same for all the models. Legend as in Fig. 5.2

a simulated temporal guess-pattern. The results of the application of the two methods to the detection of a temperature change (Sect. 5.4), also show the greater efficiency of the TOD method at detecting a signal of change when it is present.

We thus first investigate the detection of an annual precipitation change over the region using the TOD method for periods of time of varying lengths, all starting in 1900 and ending between 1920 and 2004. As a first step of the method, the temporal guess-pattern needs to be inferred from AOGCMs simulations (see Sect. 5.2). We show in Fig. 5.10 the results of the adjustment over the 1900–2004 period and each of the AOGCMs, using the averaged annual global mean temperature. These patterns are similar to those reproduced in Fig. 5.3 with a slightly different smoothing parameter.

As a second step of the TOD method, the Hotelling test is then applied using these temporal guess-patterns and the precipitation observations at the 17 coastal stations. The *p*-values of the detection test are presented on a neperian logarithmic scale with an indication of the 5% significance level. We can see in Fig. 5.11 that the 5% significance level of the detection is only episodically reached with some of the AOGCMs during the 1990s. We can thus conclude that the applied method fails at detecting a signal of climate change that cannot be explained by internal climate variability.

The *p*-values corresponding to the application of the TOD detection test are also presented for the winter and summer precipitation in Fig. 5.12. Here again, the threshold corresponding to the 5% significance level of the detection is only mar-

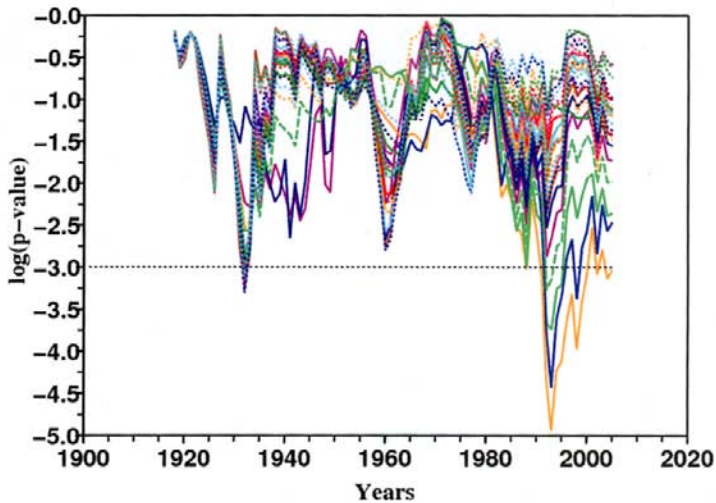


**Fig. 5.11** Detection of annual mean precipitation change over the 17 coastal stations with the TOD method using temporal guess-patterns of global mean temperature; the guess patterns are adjusted from the global mean temperatures simulated by 24 AOGCMs; the p-values of the TOD detection statistical test are presented in neperian logarithmic scale for each AOGCM; the value for 1 year corresponds to the treatment of the annual mean precipitation over a period starting at 1900 and ending this specific year; the hatched horizontal line corresponds to a p-value of 0.05 implying a 5% significance level of the detection. Legend as in Fig. 5.2

ginally exceeded and we cannot reject the null hypothesis attributing the observed change only to internal climate variability. We observe a trend towards lower p-values for periods including years of the two last decades for summer precipitation. But this result is not sufficient to conclude to the detection of a signal since the p-values remain generally greater than the 5% significance level. Note that the conclusions are identical when the TOD detection test is applied to centered mean annual, winter and summer precipitation, that is to say after the removal, at each time, of the spatial averages over the 17 series (not shown). This implies that we cannot detect a signal neither when accounting for the change in the mean spatial precipitation nor when it is excluded.

The application of the ROF detection test is more challenging as stated before. Unsurprisingly, the result of the application of this test fails at detecting a signal of climate change on annual, winter and summer precipitation (not shown).

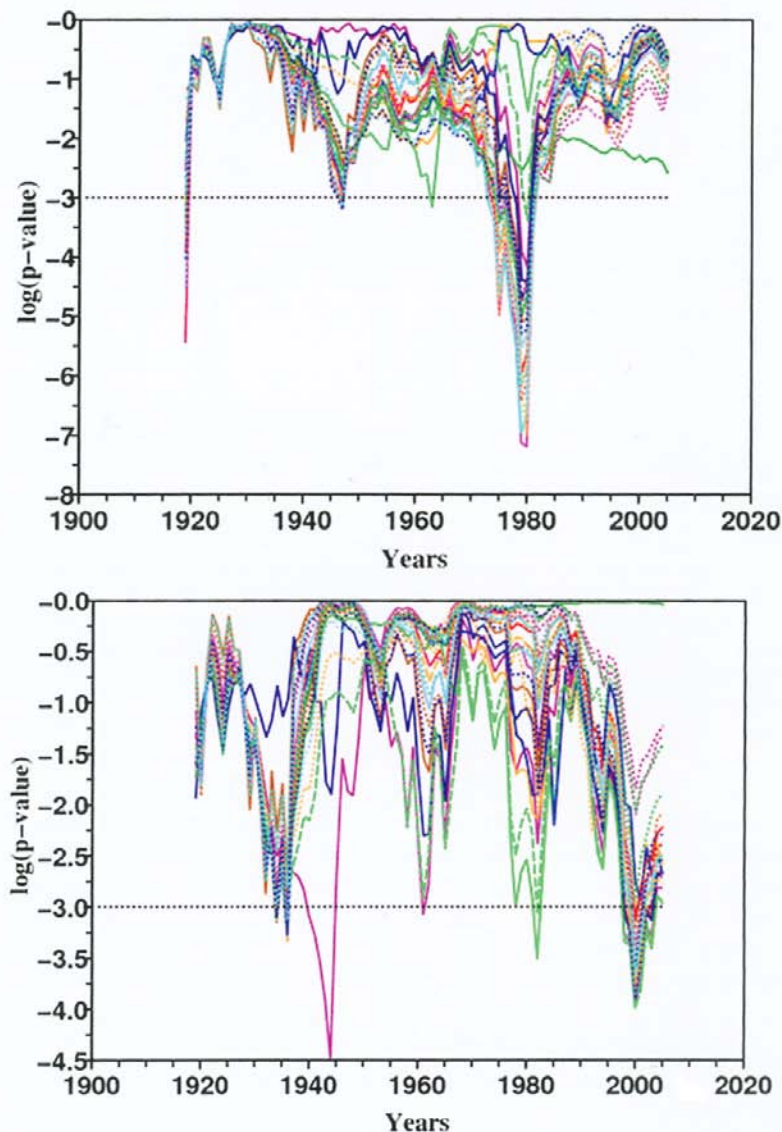


Fig. 5.12 Same as Fig. 5.10 but for winter (*top*) and summer (*bottom*) precipitation. Legend as in Fig. 5.2

## 5.6 Conclusion

We have given in this chapter a first assessment of the detection of a signal of temperature change over the Mediterranean domain, using HadCRUT3v observation dataset and model outputs from the CMIP3 climate change modeling exercise. For

this study we have used new formal detection methodologies developed within the context of the CIRCE project, in order to improve the ability to detect a climate change signal at the regional scale. These two methodologies are aimed at detecting a signal in the spatial distribution of climate change. The first one, called the ‘Regularized Optimal Fingerprint’ or ROF method allows to apply a detection test given a spatial guess-pattern of climate change provided by an ensemble of AOGCMs future scenario simulations. The second one, called the ‘Temporal Optimal Detection’ or TOD method, allows to apply a detection test given a temporal guess-pattern of climate change also provided by an ensemble of AOGCMs simulations but covering the period 1900–2006. The spatial pattern of climate change is in this case inferred from the detection test. We have also applied the ‘Consistency’ method, which focuses on the question whether the recent warming is a plausible harbinger of future warming – that is, we analyze whether the observed changes are consistent with climate change projections.

The application of the two formal detection methods on annual mean temperature reveals a detection at the 5% significance level with the most part of the AOGCMs. The TOD method is even more conclusive for this detection since the rejection of the null hypothesis is stronger and occurs with more guess-patterns than when applying the ROF method. The spatial pattern of climate change inferred from the TOD method is likely mainly of anthropogenic origin but further investigation with attribution methodologies is required to confirm this hypothesis. The application of the TOD method to winter mean temperature shows the detection of a climate change signal at the 5% significance level when considering periods covering at least the 1900–1980 period and for the most part of the CMIP3 ensemble. The same detection occurs earlier for summer mean temperatures and the significance level decreases for the longest periods. Many spatial guess-patterns of changes are also detected on summer mean temperature with the ROF method at the 5% significance level.

The application of the ‘Consistency’ method not surprisingly corroborates these results since we find that the observed warming over the Mediterranean is significantly (at 2.5% level) consistent with the response to GS forcing as derived from the 23 models. Using observationally based estimate of non-GS variability, internal variability plus other unaccounted factors, we can detect externally forced changes in the observed annual area-mean warming and in all seasons except in winter (with a probability of error of less than 5%). The consistency of observed and projected warming in area-mean quantities is largely confirmed when looking at spatially explicit pattern correlation statistics. Both with un-centered pattern correlation as well as with regression, we find generally high similarities of the patterns of observed and projected warming, which can hardly be explained as result of the ‘non-GS’ variability. Indeed it gives evidence that the large-scale component (spatial-mean) of GS-forcing has an important and dominant influence on recently observed warming trends. In contrast, we cannot explain the spatial anomalies of the warming patterns with GS-forcing. This is either due to the masking of small-scale features of the GS signal by other non-GS variability or that the spatial anomaly pattern derived from global climate model simulations is considerably flawed

due to the models' coarse horizontal resolution. It is however worth noting that the ROF method leads to the detection of the centered part of the signal for many AOGCMs for the annual and summer mean temperature due to the application of a different statistical test with a different estimate of internal climate variability.

This ensemble of results extends previous ones obtained by the application of formal detection procedures to so-called 'southern Europe' domains. These domains indeed only differ from the chosen Mediterranean domain by  $5^{\circ}$ – $10^{\circ}$  at their southern boundaries. The extension comes primarily from the detection of a change on spatially centered temperatures, that allows to identify a regional structure of change additionally to the global warming inferred by the TOD method. The extension also comes from the confirmation of the formal detection on spatial patterns of change in annual mean temperature with a much larger ensemble of large-scale AOGCM simulations, and from the extension of the formal detection findings for the winter and summer spatial patterns of temperature change.

We have also given in this chapter a first assessment of the detection of a signal of precipitation change over the Mediterranean domain, using a few long time series of observations homogenized in the context of the CIRCE project, existing precipitation databases covering the Mediterranean area, and model outputs from the CMIP3 climate change modeling exercise.

For this study we have also used the new formal detection methodologies developed within the context of the CIRCE project (ROF and TOD). The two methods are applied to the long time series of precipitation from 17 Croatian, French and Italian coastal stations, as well for annual means as for winter and summer means. The climate simulations of past and future climate are those of the 24 models stored in the CMIP3 database. The application of the two formal detection methods to annual, winter and summer precipitation don't allow to reject the null hypothesis saying that the observed changes are due to internal climate variability. The threshold of the detection test is too rarely exceeded to confirm the detection of a signal of climate change. With the application of the TOD method to summer precipitation, we observe a trend towards lower p-values for periods including the two last decades. But this result is not sufficient to state that a signal is detected since the p-values remain too high compared to the 5% significance level.

The main conclusion of this study concerning precipitation is thus that we cannot formally detect a signal of climate change on Mediterranean precipitation collected at a few locations of the Northern Mediterranean coast. Rejection of the formal detection with the dataset of the coastal stations shows that at least until now, if a climate change signal is existing, it is dominated by internal climate variability. However, it is important to note that the region covered by the homogenized series is of limited extension. This implies that we are looking for a sub-regional signal that might be poorly reproduced with current AOGCMs simulations. These results need thus to be revisited when a wider set of homogenized data will become available and with higher resolution simulations that might better reproduce an expected signal of climate change. In addition, the Mediterranean climate is affected by several tropical and subtropical systems that lead to complex features in the Mediterranean climate variability. A large number of studies refer to the role of the

NAO (North Atlantic Oscillation) on winter precipitation in the western Mediterranean and the ENSO (El Niño Southern Oscillation) has also been found also to play an important role in winter rainfall in the eastern Mediterranean (Lionello et al. 2006). Considering the effect of these processes might also give a new insight on our conclusions.

**Acknowledgments** We thank E. Xoplaki, J. Luterbacher, A. Toreti and F.G. Kuglitsch for homogenized monthly series of precipitation.

## References

- Allen MR, Stott PA (2003) Estimating signal amplitudes in optimal fingerprinting. Part I: Theory. *Clim Dyn* 21:477–491
- Barkhordarian A, Bhend J, von Storch H (2012) Consistency of observed near surface temperature trends with climate change projections over the Mediterranean region. *Clim Dyn* 38(9–10):1695–1702
- Bhend J, von Storch H (2008) Consistency of observed winter precipitation trends in northern Europe with regional climate change projections. *Clim Dyn* 31:17–28
- Bhend J, von Storch H (2009) Is greenhouse gas forcing a plausible explanation for the observed warming in the Baltic Sea catchments area? *Boreal Environ Res* 14:81–88
- Brohan P, Kennedy JJ, Harris I, Tett SFB, Jones PD (2006) Uncertainty estimates in regional and global observed temperature changes: a new data set from 1850. *J Geophys Res* 111:D12106
- Hasselmann K (1993) Optimal fingerprints for the detection of time-dependent climate change. *J Climate* 6:1957–1971
- Hegerl GC, Zwiers FW, Braconnot P, Gillett NP, Luo Y, Marengo Orsini JA, Nicholls N, Penner JE, Stott PA (2007) Understanding and attributing climate change. In: Solomon S, Qin D, Manning M, Chen Z, Marquis M, Averyt KB, Tignor M, Miller HL (eds) *Climate change 2007: the physical science basis, contribution of working group I to the fourth assessment report of the Intergovernmental Panel on Climate Change*. Cambridge University Press, Cambridge/New York, pp 663–745
- IPCC (2001) *Climate change 2001: the scientific basis. Contribution of working group I to the third assessment report of the Intergovernmental Panel on Climate Change*. Cambridge University Press, Cambridge/New York
- IPCC (2007) *Climate change 2007: the physical science basis, contribution of working group I to the fourth assessment report of the Intergovernmental Panel on Climate Change*. Cambridge University Press, Cambridge/New York, pp 663–745
- Jones PD, Osborn TJ, Briffa KR, Folland CK, Horton EB, Alexander LV, Parker DE, Rayner NA (2001) Adjusting for sampling density in grid box land and ocean surface temperature time series. *J Geophys Res* 106:3371–3380
- Kuglitsch FG, Toreti A, Xoplaki E, Della-Marta PM, Luterbacher J, Wanner H (2009) Homogenization of daily maximum temperature series in the Mediterranean. *J Geophys Res* 114:D15
- Lionello P, Malanotte-Rizzoli P, Boscolo R, Alpert P, Artale V, Li L, Luterbacher J, May W, Trigo R, Tsimplis M, Ulbrich U, Xoplaki E (2006) Mediterranean climate variability over the last centuries. In: Lionello P, Malanotte-Rizzoli P, Boscolo R (eds) *The Mediterranean climate: an overview of the main characteristics and issues*. Elsevier, Amsterdam, pp 1–26
- Ribes A, Azaïs J-M, Planton S (2009) Adaptation of the optimal fingerprint method for climate change detection using a well-conditioned covariance matrix estimate. *Clim Dyn* 33:707–722
- Ribes A, Azaïs J-M, Planton S (2010) A method for regional climate change detection using smooth temporal patterns. *Clim Dyn* 35(2–3):391–406

- Santer BD, Wigley TML, Jones PD (1993) Correlation methods in fingerprint detection studies. *Clim Dyn* 8(6):265–276
- Stott PA, Stone DA, Allen MR (2004) Human contribution to the European heat wave of 2003. *Nature* 432:610–614
- von Storch H, Zwiers F (1999) *Statistical analysis in climate research*. Cambridge University Press, Cambridge
- Wilks DS (1997) Resampling hypothesis tests for autocorrelated fields. *J Climate* 10(1):65–82
- Zhang X, Zwiers FW, Stott PA (2006) Multimodel multisignal climate change detection at regional scale. *J Climate* 19:4294–4307
- Zhang X, Zwiers FW, Hegerl GC, Lambert FH, Gillett NP, Solomon S, Stott PA, Nozawa T (2007) Detection of human influence on twentieth-century precipitation trends. *Nature* 448:461–465